View metadata, citation and similar papers at core.ac.uk

brought to you by CORE

provided by Northumbria Research Link

Northumbria Research Link

Citation: Thai, Huu-Tai, Nguyen, Trung-Kien, Vo, Thuc and Ngo, Tuan (2017) A new simple shear deformation plate theory. Composite Structures, 171. pp. 277-285. ISSN 0263-8223

Published by: Elsevier

URL: https://doi.org/10.1016/j.compstruct.2017.03.027 <https://doi.org/10.1016/j.compstruct.2017.03.027>

This version was downloaded from Northumbria Research Link: http://nrl.northumbria.ac.uk/30401/

Northumbria University has developed Northumbria Research Link (NRL) to enable users to access the University's research output. Copyright © and moral rights for items on NRL are retained by the individual author(s) and/or other copyright owners. Single copies of full items can be reproduced, displayed or performed, and given to third parties in any format or medium for personal research or study, educational, or not-for-profit purposes without prior permission or charge, provided the authors, title and full bibliographic details are given, as well as a hyperlink and/or URL to the original metadata page. The content must not be changed in any way. Full items must not be sold commercially in any format or medium without formal permission of the copyright holder. The full policy is available online: http://nrl.northumbria.ac.uk/policies.html

This document may differ from the final, published version of the research and has been made available online in accordance with publisher policies. To read and/or cite from the published version of the research, please visit the publisher's website (a subscription may be required.)

www.northumbria.ac.uk/nrl

northumbria UNIVERSITY NEWCASTLE

A new simple shear deformation plate theory

Huu-Tai Thai [a,*], Trung-Kien Nguyen [b], Thuc P. Vo [c], Tuan Ngo [d]

[a]School of Engineering and Mathematical Sciences, La Trobe University, Bundoora, VIC 3086, Australia

[b]Faculty of Civil Engineering, Ho Chi Minh City University of Technology and Education, 1 Vo Van Ngan Street, Thu Duc District, Ho Chi Minh City, Vietnam

[c]Faculty of Engineering and Environment, Northumbria University, Newcastle upon Tyne, NE1 8ST, UK

[d] Department of Infrastructure Engineering, The University of Melbourne, Parkville, VIC 3010, Australia

Abstract

This paper proposes a new simple shear deformation theory for isotropic plates. The present theory involves one unknown and one governing equation as in the classical plate theory, but it is capable of accurately capturing shear deformation effects. The displacement field of the present theory was based on a two variable refined plate theory in which the transverse displacement is partitioned into the bending and shear parts. Based on the equilibrium equations of three-dimensional (3D) elasticity theory, the relationship between the bending and shear parts was established. Therefore, the number of unknowns of the present theory was reduced from two to one. Closed-form solutions were presented for both Navier- and Levy-type plates. Numerical results indicate that the obtained predictions are comparable with those generated by ABAQUS and available results predicted by 3D elasticity theory, first-order and third-order shear deformation theories.

Keywords: Shear deformation theory; isotropic plate; analytical solution

* Corresponding author. Tel.: + 61 3 9479 3721.
E-mail address: tai.thai@latrobe.edu.au (H.T. Thai).

1. Introduction

Plates and shells are common structural elements in civil engineering structures such as buildings, bridges, tunnels, retaining walls and other infrastructure. In general, the behaviour of plate and shell structures can be predicted using either 2D plate theories or 3D elasticity theory. The classical plate theory (CPT) is the simplest plate theory developed by Love [1] based on the assumptions proposed by Kirchhoff [2]. However, this theory is only applicable for thin plates in which the shear deformation effects are negligibly small. For thick plates, the CPT underestimates deflections and overestimates buckling loads as well as natural frequencies because of neglecting these effects.

A large number of shear deformation theories have been proposed to take into account the shear deformation effects. One of the earliest shear deformation theories was proposed by Reissner [3] and Mindlin [4]. It should be noted that Mindlin's theory was based on an assumption of a linear displacement variation across the plate thickness. It was therefore referred to as the first-order shear deformation theory (FSDT). This assumption leads to constant transverse shear strains and transverse shear stresses across the thickness. A shear correction factor is therefore needed to account for the discrepancy between the constant shear stresses and the parabolic distribution of shear stresses in the 3D elasticity theory. On the other hand, Reissner's theory was based on the assumptions of a linear variation of bending stresses and a parabolic distribution of transverse shear stresses across the thickness. These assumptions lead to a displacement field which is not necessarily linear across the thickness, and the shear correction factor is not required as in the case of Mindlin's theory. Higher-order shear deformation theories (HSDTs) were proposed to eliminate the use of the shear correction factor in the FSDT, and to obtain a better prediction of the responses of very thick plates. The

HSDT is developed based on a higher-order displacement variation across the plate thickness using either polynomial functions (e.g. the third-order shear deformation theory (TSDT) of Reddy [5]) or non-polynomial functions (e.g. the sinusoidal theory of Touratier [6], hyperbolic theory of Soldatos [7], exponential theory of Karama et al. [8] and among others). Several typical shear deformation theories developed from 2010 for composite structures can be found in Refs. [9-24]. A comprehensive review of plate theories was reported by Ghugal and Shimpi [25] for isotropic and laminated plates and Thai and Kim [26] for functionally graded plates.

Although the existing HSDTs provide a better prediction compared with the CPT, they are much more complicated and computationally expensive than the CPT because of introducing additional dependent unknowns into the theory. Therefore, this paper aims to propose a simple HSDT which contains the same number of unknowns and governing equations of motion as in the case of the CPT. The present theory was based on the refined plate theory (RPT) of Shimpi [27] and 3D elasticity theory. Analytical solutions of the present theory were also presented. The obtained predictions were then compared with the available results predicted by the FSDT, TSDT and 3D elasticity theory as well as those generated by ABAQUS for validation.

2. Kinematics

The displacement field of the present theory was derived based on the displacement field of the RPT [27] and the equilibrium equations of 3D elasticity theory. According to Shimpi [27], the displacement field of the RPT is given as follows:

$$u(x,y,z,t) = -z\frac{\partial w_b}{\partial x} - z\left[\frac{5}{3}\left(\frac{z}{h}\right)^2 - \frac{1}{4}\right]\frac{\partial w_s}{\partial x} \tag{1a}$$

$$v(x,y,z,t) = -z\frac{\partial w_b}{\partial y} - z\left[\frac{5}{3}\left(\frac{z}{h}\right)^2 - \frac{1}{4}\right]\frac{\partial w_s}{\partial y} \tag{1b}$$

$$w(x,y,z,t) = w_b(x,y,t) + w_s(x,y,t) \tag{1c}$$

where (u,v,w) are the total displacement along the coordinates (x,y,z); w_b and w_s are the bending and shear components of transverse displacement *w*, respectively; and h is the plate thickness. The equilibrium equations of 3D elasticity theory in the absence of body forces are written as:

$$\frac{\partial \sigma_x}{\partial x} + \frac{\partial \sigma_{xy}}{\partial y} + \frac{\partial \sigma_{xz}}{\partial z} = \rho\ddot{u} \tag{2a}$$

$$\frac{\partial \sigma_{xy}}{\partial x} + \frac{\partial \sigma_y}{\partial y} + \frac{\partial \sigma_{yz}}{\partial z} = \rho\ddot{v} \tag{2b}$$

$$\frac{\partial \sigma_{xz}}{\partial x} + \frac{\partial \sigma_{yz}}{\partial y} + \frac{\partial \sigma_z}{\partial z} = \rho\ddot{w} \tag{2c}$$

where the dot-superscript convention indicates differentiation with respect to time t; σ_i are the stress components of the stress tensor; and ρ is the density. Substituting Eq. (1) into Eq. (2), the equilibrium equations are rewritten as:

$$\frac{\partial \sigma_x}{\partial x} + \frac{\partial \sigma_{xy}}{\partial y} + \frac{\partial \sigma_{xz}}{\partial z} = -\rho z\frac{\partial \ddot{w}_b}{\partial x} - \rho z\left[\frac{5}{3}\left(\frac{z}{h}\right)^2 - \frac{1}{4}\right]\frac{\partial \ddot{w}_s}{\partial x} \tag{3a}$$

$$\frac{\partial \sigma_{xy}}{\partial x} + \frac{\partial \sigma_y}{\partial y} + \frac{\partial \sigma_{yz}}{\partial z} = -\rho z\frac{\partial \ddot{w}_b}{\partial y} - \rho z\left[\frac{5}{3}\left(\frac{z}{h}\right)^2 - \frac{1}{4}\right]\frac{\partial \ddot{w}_s}{\partial y} \tag{3b}$$

$$\frac{\partial \sigma_{xz}}{\partial x} + \frac{\partial \sigma_{yz}}{\partial y} + \frac{\partial \sigma_z}{\partial z} = \rho\left(\ddot{w}_b + \ddot{w}_s\right) \tag{3c}$$

The equilibrium equations in Eq. (3) can be rewritten in terms of stress resultants for a plate under a transversely distributed load *q* as shown in Fig. 1 by multiplying the first two equations by *z* and then integrating all three equations with respect to *z*, and

applying several boundary conditions, i.e. the transverse shear stresses σ_{xz} and σ_{yz} equal to zero at $z = \pm h/2$ and the normal stress through the thickness $\sigma_z = 0$ at $z = -h/2$ and $\sigma_z = -q$ at $z = h/2$. The resulting equations are:

$$\frac{\partial M_x}{\partial x} + \frac{\partial M_{xy}}{\partial y} - Q_x = -I_2 \frac{\partial \ddot{w}_b}{\partial x} \tag{4a}$$

$$\frac{\partial M_{xy}}{\partial x} + \frac{\partial M_y}{\partial y} - Q_y = -I_2 \frac{\partial \ddot{w}_b}{\partial y} \tag{4b}$$

$$\frac{\partial Q_x}{\partial x} + \frac{\partial Q_y}{\partial y} + q = I_0 \left(\ddot{w}_b + \ddot{w}_s \right) \tag{4c}$$

where the moments *M*, shear forces *Q* and mass inertias *I* are defined as

$$M_x = \int_{-h/2}^{h/2} z\sigma_x dz \tag{5a}$$

$$M_y = \int_{-h/2}^{h/2} z\sigma_y dz \tag{5b}$$

$$M_{xy} = \int_{-h/2}^{h/2} z\sigma_{xy} dz \tag{5c}$$

$$Q_x = \int_{-h/2}^{h/2} \sigma_{xz} dz \tag{6a}$$

$$Q_y = \int_{-h/2}^{h/2} \sigma_{yz} dz \tag{6b}$$

$$I_0 = \int_{-h/2}^{h/2} \rho dz \tag{7a}$$

$$I_2 = \int_{-h/2}^{h/2} \rho z^2 dz \tag{7b}$$

According to Shimpi [27], the moments and shear forces can be expressed in terms of

the dependent unknowns (w_b, w_s) as

$$M_x = -D\left(\frac{\partial^2 w_b}{\partial x^2} + \nu \frac{\partial^2 w_b}{\partial y^2}\right) \tag{8a}$$

$$M_y = -D\left(\frac{\partial^2 w_b}{\partial y^2} + \nu \frac{\partial^2 w_b}{\partial x^2}\right) \tag{8b}$$

$$M_{xy} = -D(1-\nu)\frac{\partial^2 w_b}{\partial x \partial y} \tag{8c}$$

$$Q_x = A_s \frac{\partial w_s}{\partial x} \tag{9a}$$

$$Q_y = A_s \frac{\partial w_s}{\partial y} \tag{9b}$$

where

$$D = \frac{Eh^3}{12(1-\nu^2)} \quad \text{and} \quad A_s = \frac{5Eh}{12(1+\nu)} \tag{10}$$

where E and ν are the Young's modulus and Poisson's ratio of isotropic materials, respectively. Substituting Eqs. (8) and (9) into Eq. (4a) or Eq. (4b), the relationship between the bending component w_b and shear component w_s is obtained as:

$$w_s = \frac{I_2}{A_s}\ddot{w}_b - \frac{D}{A_s}\nabla^2 w_b \tag{11}$$

where $\nabla^2 = \frac{\partial^2}{\partial x^2} + \frac{\partial^2}{\partial y^2}$. The displacement field of the present theory can be obtained by substituting Eq. (11) into Eq. (1):

$$u(x,y,z,t) = -z\frac{\partial w_b}{\partial x} \underline{-z\left[\frac{5}{3}\left(\frac{z}{h}\right)^2 - \frac{1}{4}\right]\left[\frac{I_2}{A_s}\frac{\partial \ddot{w}_b}{\partial x} - \frac{D}{A_s}\nabla^2\left(\frac{\partial w_b}{\partial x}\right)\right]} \tag{12a}$$

$$v(x,y,z,t) = -z\frac{\partial w_b}{\partial y} \underline{-z\left[\frac{5}{3}\left(\frac{z}{h}\right)^2 - \frac{1}{4}\right]\left[\frac{I_2}{A_s}\frac{\partial \ddot{w}_b}{\partial y} - \frac{D}{A_s}\nabla^2\left(\frac{\partial w_b}{\partial y}\right)\right]} \tag{12b}$$

$$w(x,y,z,t) = w_b \underline{- \frac{D}{A_s}\nabla^2 w_b + \frac{I_2}{A_s}\ddot{w}_b} \tag{12c}$$

It can be seen from Eq. (12) that the displacement field of the present theory involves only one unknown w_b. If the underlined terms in Eq. (12) are neglected, the present theory becomes the CPT.

3. Governing equations of motion

Substituting Eqs. (4a) and (4b) into Eq. (4c), the equations of motion of the present theory is obtained from the equilibrium equations of 3D elasticity theory as:

$$\frac{\partial^2 M_x}{\partial x^2} + 2\frac{\partial^2 M_{xy}}{\partial x \partial y} + \frac{\partial^2 M_y}{\partial y^2} + q = I_0\left(\ddot{w}_b + \ddot{w}_s\right) - I_2\nabla^2\ddot{w}_b \tag{13}$$

Eq. (13) can be expressed in terms of the displacement w_b by substituting Eqs. (8) and (11) into Eq. (13):

$$-D\nabla^4 w_b + q = I_0\ddot{w}_b - \left(I_2 + \frac{I_0 D}{A_s}\right)\nabla^2\ddot{w}_b + \frac{I_0 I_2}{A_s}\ddot{\ddot{w}}_b \tag{14}$$

where $\nabla^4 = \frac{\partial^4}{\partial x^4} + 2\frac{\partial^4}{\partial x^2 \partial y^2} + \frac{\partial^4}{\partial y^4}$. For a static analysis, Eq. (14) was simplified as:

$$D\nabla^4 w_b = q \tag{15}$$

Eq. (15) is similar to the governing equation of the CPT. The only difference is that the governing equation of the present theory involves the bending component w_b of the transverse displacement instead of the total transverse displacement *w* as in the case of the CPT. The boundary conditions of the present theory are in a similar form as the CPT as [27]:

For free edges:

$$M_x = 0 \quad \text{and} \quad V_x \equiv Q_x + \frac{\partial M_{xy}}{\partial y} = 0 \quad \text{on the edges} \quad x = 0, a \tag{16a}$$

$$M_y = 0 \quad \text{and} \quad V_y \equiv Q_y + \frac{\partial M_{xy}}{\partial x} = 0 \quad \text{on the edges} \quad y = 0, b \tag{16b}$$

For simply supported edges:

$$w = 0 \quad \text{and} \quad M_x = 0 \quad \text{on the edges} \quad x = 0, a \tag{17a}$$

$$w = 0 \quad \text{and} \quad M_y = 0 \quad \text{on the edges} \quad y = 0, b \tag{17b}$$

For clamped edges, there are two possible types of clamped boundary conditions as mentioned in [27]:

$$w = 0 \quad \text{and} \quad \frac{\partial w}{\partial x} = 0 \quad \text{on the edges} \quad x = 0, a \tag{18a}$$

$$w = 0 \quad \text{and} \quad \frac{\partial w}{\partial y} = 0 \quad \text{on the edges} \quad y = 0, b \tag{18b}$$

or

$$w = 0 \quad \text{and} \quad \left.\frac{\partial u}{\partial z}\right|_{z=0} = 0 \quad \text{on the edges} \quad x = 0, a \tag{19a}$$

$$w = 0 \quad \text{and} \quad \left.\frac{\partial v}{\partial z}\right|_{z=0} = 0 \quad \text{on the edges} \quad y = 0, b \tag{19b}$$

4. Analytical solutions

4.1. Navier-type plates

Consider a Navier-type plate subjected to a transverse load q as shown in Fig. 1. The expansion of w_b which satisfies the simply supported boundary conditions of the Navier-type plate was selected as follows:

$$w_b(x, y, t) = \sum_{m=1}^{\infty}\sum_{n=1}^{\infty} W_{bmn} e^{i\omega t} \sin \alpha x \sin \beta y \tag{20}$$

where $\alpha = m\pi / a$; $\beta = n\pi / b$; ω is the natural frequency; and W_{bmn} are coefficients. The transversely distributed load q can be also expressed as:

$$q(x,y) = \sum_{m=1}^{\infty}\sum_{n=1}^{\infty} Q_{mn} \sin\alpha x \sin\beta y \tag{21}$$

where

$$Q_{mn} = \frac{4}{ab}\int_0^a\int_0^b q(x,y)\sin\alpha x \sin\beta y dx dy = \begin{cases} q_0 \text{ for sinusoidally distributed load} \\ \dfrac{16q_0}{mn\pi^2} \text{ for uniformly distributed load} \end{cases} \tag{22}$$

Substituting Eqs. (20) and (21) into Eq. (14), the following equation is obtained

$$\left\{ D\left(\alpha^2+\beta^2\right)^2 - \omega^2\left[I_0 + \left(I_2 + \frac{I_0 D}{A_s}\right)\left(\alpha^2+\beta^2\right)\right] + \frac{I_0 I_2}{A_s}\omega^4 \right\} W_{bmn} = Q_{mn} \tag{23}$$

For a static analysis ($\omega = 0$), the analytical solution of the bending component w_b is obtained as:

$$w_b = \sum_{m=1}^{\infty}\sum_{n=1}^{\infty} \frac{Q_{mn}}{D\left(\alpha^2+\beta^2\right)^2} \sin\alpha x \sin\beta y \tag{24}$$

The closed-form solutions for the deflections *w*, stresses σ, bending moments *M* and shear forces *Q* are subsequently obtained based on w_b as follows:

$$w = \sum_{m=1}^{\infty}\sum_{n=1}^{\infty}\left[1 + \underline{\frac{D}{A_s}\left(\alpha^2+\beta^2\right)}\right] \frac{Q_{mn}}{D\left(\alpha^2+\beta^2\right)^2} \sin\alpha x \sin\beta y \tag{25}$$

$$\sigma_x = \frac{Ez}{1-\nu^2}\sum_{m=1}^{\infty}\sum_{n=1}^{\infty}\left[1 + \underline{\frac{D}{A_s}\left(\alpha^2+\beta^2\right)\left(\frac{5z^2}{3h^2} - \frac{1}{4}\right)}\right] \frac{\left(\alpha^2+\nu\beta^2\right)Q_{mn}}{D\left(\alpha^2+\beta^2\right)^2} \sin\alpha x \sin\beta y \tag{26a}$$

$$\sigma_y = \frac{Ez}{1-\nu^2}\sum_{m=1}^{\infty}\sum_{n=1}^{\infty}\left[1 + \underline{\frac{D}{A_s}\left(\alpha^2+\beta^2\right)\left(\frac{5z^2}{3h^2} - \frac{1}{4}\right)}\right] \frac{\left(\nu\alpha^2+\beta^2\right)Q_{mn}}{D\left(\alpha^2+\beta^2\right)^2} \sin\alpha x \sin\beta y \tag{26b}$$

$$\sigma_{xy} = \frac{Ez}{1+\nu}\sum_{m=1}^{\infty}\sum_{n=1}^{\infty}\left[1+\underline{\frac{D}{A_s}\left(\alpha^2+\beta^2\right)\left(\frac{5z^2}{3h^2}-\frac{1}{4}\right)}\right]\frac{\alpha\beta Q_{mn}}{D\left(\alpha^2+\beta^2\right)^2}\cos\alpha x\cos\beta y \quad (26c)$$

$$\sigma_{xz} = \frac{6}{h}\left(\frac{1}{4}-\frac{z^2}{h^2}\right)\sum_{m=1}^{\infty}\sum_{n=1}^{\infty}\frac{\alpha Q_{mn}}{\alpha^2+\beta^2}\cos\alpha x\sin\beta y \quad (26d)$$

$$\sigma_{yz} = \frac{6}{h}\left(\frac{1}{4}-\frac{z^2}{h^2}\right)\sum_{m=1}^{\infty}\sum_{n=1}^{\infty}\frac{\beta Q_{mn}}{\alpha^2+\beta^2}\sin\alpha x\cos\beta y \quad (26e)$$

$$M_x = \sum_{m=1}^{\infty}\sum_{n=1}^{\infty}\frac{\left(\alpha^2+\nu\beta^2\right)Q_{mn}}{\left(\alpha^2+\beta^2\right)^2}\sin\alpha x\sin\beta y \quad (27a)$$

$$M_y = \sum_{m=1}^{\infty}\sum_{n=1}^{\infty}\frac{\left(\nu\alpha^2+\beta^2\right)Q_{mn}}{\left(\alpha^2+\beta^2\right)^2}\sin\alpha x\sin\beta y \quad (27b)$$

$$M_{xy} = -(1-\nu)\sum_{m=1}^{\infty}\sum_{n=1}^{\infty}\frac{\alpha\beta Q_{mn}}{\left(\alpha^2+\beta^2\right)^2}\cos\alpha x\cos\beta y \quad (27c)$$

$$Q_x = \sum_{m=1}^{\infty}\sum_{n=1}^{\infty}\frac{\alpha Q_{mn}}{\alpha^2+\beta^2}\cos\alpha x\sin\beta y \quad (28a)$$

$$Q_y = \sum_{m=1}^{\infty}\sum_{n=1}^{\infty}\frac{\beta Q_{mn}}{\alpha^2+\beta^2}\sin\alpha x\cos\beta y \quad (28b)$$

It should be noted that the CPT does not account for the underlined terms in Eqs. (25) and (26). For a free vibration analysis ($q=0$), the analytical solution for the natural frequency ω is obtained from in Eq. (23) as:

$$\omega^2 = \frac{I_0+(I_2+\frac{I_0D}{A_s})(\alpha^2+\beta^2)-\sqrt{\left[I_0+(I_2+\frac{I_0D}{A_s})(\alpha^2+\beta^2)\right]^2-4\frac{I_0I_2D}{A_s}(\alpha^2+\beta^2)^2}}{2I_0I_2/A_s} \quad (29)$$

If the time derivative term in Eq. (11) is neglected, the natural frequency of a simply supported plate is simplified as:

$$\omega^2 = \frac{D\left(\alpha^2+\beta^2\right)^2}{I_0 + I_2\left(\alpha^2+\beta^2\right) + \underline{\frac{I_0 D}{A_s}\left(\alpha^2+\beta^2\right)}} \tag{30}$$

If the underlined shear deformation term in Eq. (30) is neglected, the natural frequency of the present theory yields the frequency obtained from the CPT. Fig. 2 illustrates the comparison between the nondimensional fundamental frequencies $\bar{\omega} = \omega a^2\sqrt{\rho h / D}$ predicted by CPT (using Eq. (30) without the underline term), FSDT given by Thai et al. [28] and the present theory with the exact and simplified formulations. It can be observed that the difference in the frequencies predicted by the exact and simplified formulations in Eqs. (29) and (30) is negligible, and the predictions of the present theory are close to those predicted by the FSDT [28].

4.2. Levy-type plates

Consider a rectangular plate with simply supported boundary conditions at the edges $x = 0, a$ and arbitrary boundary conditions at the remaining edges $y = 0, b$. The following expansion of w_b was chosen to satisfy the boundary conditions of the Levy-type plate as follows:

$$w_b\left(x, y, t\right) = \sum_{m=1}^{\infty} W_{bm}\left(y\right) e^{i\omega t} \sin\alpha x \tag{31}$$

The applied load q can be expressed as:

$$q\left(x, y\right) = \sum_{m=1}^{\infty} Q_m\left(y\right) \sin\alpha x \tag{32}$$

where

$$Q_m\left(y\right) = \frac{2}{a}\int_0^a q\left(x, y\right)\sin\alpha x dx = \begin{cases} q_0 \text{ for sinusoidally distributed load} \\ \dfrac{4q_0}{m\pi} \text{ for uniformly distributed load} \end{cases} \tag{33}$$

Substituting Eqs. (31) and (32) into the governing equations of motion Eq. (14), the

following equation is obtained:

$$W_{bm}^{\prime\prime\prime\prime} = C_1 W_{bm} + C_2 W_{bm}^{\prime\prime} + Q_m / D \tag{34}$$

where the prime notations denote the derivatives with respect to y and the coefficients C_i are define by:

$$C_1 = \frac{I_0}{D}\omega^2 + \left(\frac{I_2}{D} + \frac{I_0}{A_s}\right)\alpha^2\omega^2 - \frac{I_0 I_2}{D A_s}\omega^4 - \alpha^4,\ C_2 = 2\alpha^2 - \left(\frac{I_2}{D} + \frac{I_0}{A_s}\right)\omega^2 \tag{35}$$

For a static analysis $(\omega = 0)$, the governing equations of the present theory are similar to those of the CPT as in Eq. (15). Therefore, the analytical solution of Eq. (34) is obtained as:

$$W_{bm}(y) = (A_m + B_m y)\cosh\alpha y + (C_m + D_m y)\sinh\alpha y + \frac{Q_m}{D\alpha^4} \tag{36}$$

where the constants (A_m, B_m, C_m, D_m) can be obtained using boundary conditions at the edges $y = 0, b$. Substituting the stress resultants (M and Q) and deflection w into Eqs. (16)-(19), the boundary conditions at the edges $y = 0, b$ can be rewritten in terms of W_{bm} as

Free (F):

$$D\left(\nu\alpha^2 W_{bm} - W_{bm}^{\prime\prime}\right) = 0 \tag{37a}$$

$$\left[D(2-\nu)\alpha^2 - I_2\omega^2\right]W_{bm}^{\prime} - D W_{bm}^{\prime\prime\prime} = 0 \tag{37b}$$

Simply supported (S):

$$\left(1 + \frac{D}{A_s}\alpha^2 - \frac{I_2}{A_s}\omega^2\right)W_{bm} - \frac{D}{A_s}W_{bm}^{\prime\prime} = 0 \tag{38a}$$

$$D\left(\nu\alpha^2 W_{bm} - W_{bm}^{\prime\prime}\right) = 0 \tag{38b}$$

Clamped (C):

$$\left(1+\frac{D}{A_s}\alpha^2-\frac{I_2}{A_s}\omega^2\right)W_{bm}-\frac{D}{A_s}W_{bm}''=0 \tag{39a}$$

$$\left(1+\frac{D}{A_s}\alpha^2-\frac{I_2}{A_s}\omega^2\right)W_{bm}'-\frac{D}{A_s}W_{bm}'''=0 \tag{39b}$$

or

$$\left(1+\frac{D}{A_s}\alpha^2-\frac{I_2}{A_s}\omega^2\right)W_{bm}-\frac{D}{A_s}W_{bm}''=0 \tag{40a}$$

$$\left(-1+\frac{D}{4A_s}\alpha^2-\frac{I_2}{4A_s}\omega^2\right)W_{bm}'-\frac{D}{4A_s}W_{bm}'''=0 \tag{40b}$$

For a free vibration analysis $(q=0)$, the state-space approach can be used to solve Eq. (34) for the natural frequency. More details on the application of this approach can be found in Refs. [29-32].

5. Numerical examples

A number of examples were presented in this section to illustrate the accuracy and efficiency of the present theory and its analytical solutions. The bending response and natural frequency predicted by the present one unknown shear deformation theory were compared with available results predicted by 3D elasticity theory and well-known plate theories such as the CPT, FSDT and TSDT. It should be noted that the CPT has only a single unknown as in the case of the present theory, whilst the FSDT and TSDT involve three unknowns. In addition, the numerical solutions generated in this study using the shell element S4R of the commercial finite element software ABAQUS [33] were also used for validation. S4R is a robust quadrilateral 4-node element with reduced integration which is applicable for both thin and thick plate/shell structures. Based on a convergence study, the mesh sizes of 40×40 and 40×80 were respectively selected for

the number of element along the edges of square plates and rectangular plates with aspect ratios of 2.0.

5.1. Bending analysis

The first bending example aims to validate the present theory for Navier-type plates. Three values for the length-to-thickness ratio a/h of 5, 10 (corresponding to thick and moderately thick plates) and 100 (corresponding to thin plates) were taken into account. The obtained predictions were compared with available results reported by Reddy [34] using the CPT, FSDT, and TSDT in Table 1 in which the normalized quantities were defined as follows:

$$\begin{aligned}
&\bar{\sigma}_i = \frac{h^2}{qa^2}\sigma_i\left(\frac{a}{2},\frac{b}{2},\frac{h}{2}\right),\ (i=x,y)\\
&\bar{\sigma}_{xy} = \frac{h^2}{qa^2}\sigma_{xy}\left(0,0,\frac{h}{2}\right)\\
&\bar{\sigma}_{yz} = \frac{h}{qa}\sigma_{yz}\left(\frac{a}{2},0,0\right)\\
&\bar{\sigma}_{xz} = \frac{h}{qa}\sigma_{xz}\left(0,\frac{b}{2},0\right)\\
&\bar{w} = \frac{Eh^3}{qa^4}w\left(\frac{a}{2},\frac{b}{2}\right)
\end{aligned} \tag{41}$$

The obtained predictions were calculated using up to 19 terms in the series as performed by Reddy [34]. It should be noted that the values of the transverse shear stresses given by Reddy [34] were based on integrating the equilibrium equations of 3D elasticity theory with respect to the thickness coordinate as

$$\sigma_{xz} = -\int_{-h/2}^{z}\left(\frac{\partial\sigma_x}{\partial x}+\frac{\partial\sigma_{xy}}{\partial y}\right)dz \tag{42a}$$

$$\sigma_{yz} = -\int_{-h/2}^{z}\left(\frac{\partial\sigma_{xy}}{\partial x}+\frac{\partial\sigma_y}{\partial y}\right)dz \tag{42b}$$

It can be observed from Table 1 that the deflections and in-plane stresses obtained by

the present theory agree well with those predicted by the FSDT and TSDT. Since the shear deformation effects were included in the present theory, FSDT and TSDT, their predictions are similar each other and agree well with the finite element solutions of ABAQUS. On the contrary, the CPT underestimates deflections of thick plates because of ignoring shear deformation effects. For example, for thick plates with $a/h = 5$, the CPT underestimates the deflections by 17.10% and 11.38% for square and rectangular plates, respectively. It is also seen from Table 1 that the transverse shear stresses obtained from the present theory are identical with those predicted by the CPT and FSDT. As stated by Reddy [34], both CPT and FSDT give more accurate predictions of the transverse shear stresses than the TSDT when the stress equilibrium equations of 3D elasticity theory are used. It is also noted that the present theory has only one unknown as in the CPT, whilst both FSDT and TSDT involves three unknowns. Although the CPT can give the same accuracy in predicting the transverse shear stress as in the case of the present theory, it was based on an indirect and lengthy process through the use of equilibrium equations in Eq. (42). In contrast to the CPT, the present theory predicts the transverse shear stresses in a direct manner through the use of constitutive relations in Eqs. (26d) and (26e). It should be noted that the transverse shear stresses predicted by the CPT using constitutive relations are always equal to zero. A comparison of the variation of $\bar{w}$ with respect to a/h was also plotted in Fig. 3 for square plates. Again, an excellent agreement between the results generated by the present theory, TSDT and ABAQUS was observed.

To further illustrate the accuracy of the present theory in predicting the transverse shear stresses, Fig. 4 compared the distribution of the transverse shear stress predicted by the present theory with that given by Auricchio and Sacco [35] based on the exact 3D

elasticity solutions derived by Pagano [36]. For the plate strip under a sinusoidal load, the transverse shear stress given in Eq. (26d) was simplified as $\sigma_{xz} = \frac{6qa}{\pi h}\left(\frac{1}{4} - \frac{z^2}{h^2}\right)$. It can be seen from Fig. 4 that the obtained prediction agrees well with the exact 3D solutions. This is expected since the present theory was based on equilibrium considerations.

The next bending example aims to verify the present theory for Levy-type plates. Table 2 compared the nondimensional deflection at the centre of Levy-type plates under uniformly distributed loads. The aspect ratio is taken as 2.0, whilst the nondimensional deflection is defined as $\hat{w} = \frac{100D}{qa^4} w$ with $D = \frac{Eh^3}{12\left(1-\nu^2\right)}$. Four values of a/h of 5, 10 (corresponding to thick and moderately thick plates), 25 and 1000 (corresponding to thin plates) were considered. For the plates involving the clamped boundary conditions (CC, SC and FC plates), two types of the clamped boundary conditions described in Eqs (39) and (40) were used. The obtained solutions were compared with the available solutions of the FSDT reported by Zenkour [37] and the FE solutions of ABAQUS. The plate deformations generated by ABAQUS were also illustrated in Fig. 5 for the case of moderately thick plates with a/h = 10. In general, the deflections predicted by the present theory are in good agreement with those predicted by the FSDT and ABAQUS, except for the case of the thick CC plate with a/h = 5 where a slightly difference of 6.43% between the results was found if the clamped boundary conditions in Eq. (39) were used. However, this difference becomes negligible when the clamped boundary conditions in Eq. (40) were used. This indicated that for the plate involving the clamped boundary conditions, the boundary conditions described in Eq. (40) should be used to give a better prediction.

5.2. Free vibration analysis

The first verification for free vibration analysis was carried out for SS square plates. This example aims to verify the present theory for a wide range of Navier-type plates with a thickness-to-length ratio h/a covering from 0.001 (very thin plates) to 0.4 (very thick plates). Table 3 showed a comparison of the first eight nondimensional frequencies $\bar{\omega}$ obtained in this study with available results predicted by the CPT [38], FSDT [39], TSDT [40-41] and 3D elasticity theory [42-43]. The obtained results were also compared with the FE results computed independently in this study using ABAQUS. The first eight mode shapes generated by ABAQUS were also plotted in Fig. 6 for very thick plates with $h/a = 0.4$. It is noted that the 3D results given by Liew et al. [42] were based on the Ritz method, whilst Malik and Bert [43] used the differential quadrature (DQ) method to solve for the frequencies. The TSDT results reported by Shufrin and Eisenberger [40] were based on the extended Kantorovich numerical method, whilst Hosseini-Hashemi et al. [41] employed the Levy method to derive exact TSDT solutions. Both CPT and FSDT results given by Leissa [38] and Hosseini-Hashemi and Arsanjani [39], respectively, were based on an analytical approach. Good agreement between the results was found in Table 3 for all models of very thin to very thick plates.

The next verification for free vibration analysis aims to verify the present theory for a wide range of square and rectangular plates with various boundary conditions. Table 4 contains the nondimensional frequencies $\bar{\omega}$ of plates for various values of the thickness-to-length ratio h/a. It is noted that the frequencies of the CC, SC and FC plates were obtained based on the clamped boundary conditions described in Eq. (40) due to its accuracy. The results obtained in this study were compared with available results reported by Malik and Bert [43], Hosseini-Hashemi and Arsanjani [39] and

Hosseini-Hashemi et al. [41] based on 3D elasticity theory, FSDT and TSDT, respectively. Good agreement between the results is observed in Table 4 confirming the accuracy of the present theory.

6. Conclusions

A simple and accurate shear deformation theory has been proposed for thick isotropic plates. The governing equations of motion of the present theory were derived based on 3D elasticity theory and RPT. The accuracy of the present theory in predicting the bending behaviour and natural frequencies was verified for a wide range of Navier- and Lery-type plates. Numerical results indicated that the present theory is not only much more accurate than the CPT but also comparable with the FSDT and TSDT when compared with 3D elasticity theory and ABAQUS. Although the present theory has only one unknown and one governing equations of motion as in the CPT, its predictions are comparable with those generated by the FSDT and TSDT which have three unknowns and three governing equations.

Acknowledgements

This work in this paper was supported by the School of Engineering and Mathematical Sciences at La Trobe University. This financial support is gratefully acknowledged.

References

[1] Love AEH. The small free vibrations and deformation of a thin elastic shell. Philosophical Transactions of the Royal Society of London. A 1888;179:491-546.

[2] Kirchhoff GR. Uber das gleichgewicht und die bewegung einer elastischen scheibe.

1850;40:51-88.

[3] Reissner E. The effect of transverse shear deformation on the bending of elastic plates. Journal of Applied Mechanics 1945;12:69-72.

[4] Mindlin RD. Influence of rotatory inertia and shear on flexural motions of isotropic, elastic plates. Journal of Applied Mechanics 1951;18:31-38.

[5] Reddy JN. A simple higher-order theory for laminated composite plates. Journal of Applied Mechanics 1984;51:745-752.

[6] Touratier M. An efficient standard plate theory. International Journal of Engineering Science 1991;29:901-916.

[7] Soldatos KP. A transverse shear deformation theory for homogeneous monoclinic plates. Acta Mechanica 1992;94:195-220.

[8] Karama M, Afaq KS, Mistou S. Mechanical behaviour of laminated composite beam by the new multi-layered laminated composite structures model with transverse shear stress continuity. International Journal of Solids and Structures 2003;40:1525-1546.

[9] Ferreira AJM, Carrera E, Cinefra M, Roque CMC, Polit O. Analysis of laminated shells by a sinusoidal shear deformation theory and radial basis functions collocation, accounting for through-the-thickness deformations. Composites Part B: Engineering 2011;42:1276-1284.

[10] Mantari JL, Guedes Soares C. Generalized hybrid quasi-3D shear deformation theory for the static analysis of advanced composite plates. Composite Structures 2012;94:2561-2575.

[11] Neves AMA, Ferreira AJM, Carrera E, Cinefra M, Roque CMC, Jorge RMN, et al. A quasi-3D hyperbolic shear deformation theory for the static and free vibration

analysis of functionally graded plates. Composite Structures 2012;94:1814-1825.

[12] Neves AMA, Ferreira AJM, Carrera E, Roque CMC, Cinefra M, Jorge RMN, et al. A quasi-3D sinusoidal shear deformation theory for the static and free vibration analysis of functionally graded plates. Composites Part B: Engineering 2012;43:711-725.

[13] Neves AMA, Ferreira AJM, Carrera E, Cinefra M, Roque CMC, Jorge RMN, et al. Static, free vibration and buckling analysis of isotropic and sandwich functionally graded plates using a quasi-3D higher-order shear deformation theory and a meshless technique. Composites Part B: Engineering 2013;44:657-674.

[14] Thai HT, Choi DH. A simple first-order shear deformation theory for laminated composite plates. Composite Structures 2013;106:754-763.

[15] Thai HT, Choi DH. A simple first-order shear deformation theory for the bending and free vibration analysis of functionally graded plates. Composite Structures 2013;101:332-340.

[16] Thai HT, Kim SE. A simple quasi-3D sinusoidal shear deformation theory for functionally graded plates. Composite Structures 2013;99:172-180.

[17] Thai HT, Kim SE. A simple higher-order shear deformation theory for bending and free vibration analysis of functionally graded plates. Composite Structures 2013;96:165-173.

[18] Mantari JL, Guedes Soares C. A trigonometric plate theory with 5-unknowns and stretching effect for advanced composite plates. Composite Structures 2014;107:396-405.

[19] Mantari JL, Guedes Soares C. Four-unknown quasi-3D shear deformation theory for advanced composite plates. Composite Structures 2014;109:231-239.

[20] Mantari JL, Granados EV. A refined FSDT for the static analysis of functionally graded sandwich plates. Thin-Walled Structures 2015;90:150-158.

[21] Vo TP, Thai HT, Nguyen TK, Inam F, Lee J. A quasi-3D theory for vibration and buckling of functionally graded sandwich beams. Composite Structures 2015;119:1-12.

[22] Mantari JL, Ramos IA, Carrera E, Petrolo M. Static analysis of functionally graded plates using new non-polynomial displacement fields via Carrera Unified Formulation. Composites Part B: Engineering 2016;89:127-142.

[23] Sarangan S, Singh BN. Higher-order closed-form solution for the analysis of laminated composite and sandwich plates based on new shear deformation theories. Composite Structures 2016;138:391-403.

[24] Farzam-Rad SA, Hassani B, Karamodin A. Isogeometric analysis of functionally graded plates using a new quasi-3D shear deformation theory based on physical neutral surface. Composites Part B: Engineering 2017;108:174-189.

[25] Ghugal YM, Shimpi RP. A review of refined shear deformation theories of isotropic and anisotropic laminated plates. Journal of Reinforced Plastics and Composites 2002;21:775-813.

[26] Thai HT, Kim SE. A review of theories for the modeling and analysis of functionally graded plates and shells. Composite Structures 2015;128:70-86.

[27] Shimpi RP. Refined plate theory and its variants. AIAA Journal 2002;40:137-146.

[28] Thai HT, Park M, Choi DH. A simple refined theory for bending, buckling, and vibration of thick plates resting on elastic foundation. International Journal of Mechanical Sciences 2013;73:40-52.

[29] Thai HT, Kim SE. Levy-type solution for buckling analysis of orthotropic plates

based on two variable refined plate theory. Composite Structures 2011;93:1738-1746.

[30] Thai HT, Kim SE. Levy-type solution for free vibration analysis of orthotropic plates based on two variable refined plate theory. Applied Mathematical Modelling 2012;36:3870-3882.

[31] Thai HT, Kim SE. Analytical solution of a two variable refined plate theory for bending analysis of orthotropic Levy-type plates. International Journal of Mechanical Sciences 2012;54:269-276.

[32] Thai HT, Choi DH. Analytical solutions of refined plate theory for bending, buckling and vibration analyses of thick plates. Applied Mathematical Modelling 2013;37:8310-8323.

[33] ABAQUS. Standard user's manual, version 6.15: Dassault Systemes Corp., Providence, RI (USA); 2016.

[34] Reddy JN. A refined nonlinear theory of plates with transverse shear deformation. International Journal of Solids and Structures 1984;20:881-896.

[35] Auricchio F, Sacco E. Refined first-order shear deformation theory models for composite laminates. Journal of Applied Mechanics 2003;70:381-390.

[36] Pagano N. Exact solutions for composite laminates in cylindrical bending. Mechanics of Composite Materials: Springer; 1994. p. 72-85.

[37] Zenkour AM. Exact mixed-classical solutions for the bending analysis of shear deformable rectangular plates. Applied Mathematical Modelling 2003;27:515-534.

[38] Leissa AW. The free vibration of rectangular plates. Journal of Sound and Vibration 1973;31:257-293.

[39] Hosseini-Hashemi S, Arsanjani M. Exact characteristic equations for some of

classical boundary conditions of vibrating moderately thick rectangular plates. International Journal of Solids and Structures 2005;42:819-853.

[40] Shufrin I, Eisenberger M. Stability and vibration of shear deformable plates—first order and higher order analyses. International Journal of Solids and Structures 2005;42:1225-1251.

[41] Hosseini-Hashemi S, Fadaee M, Rokni Damavandi Taher H. Exact solutions for free flexural vibration of Levy-type rectangular thick plates via third-order shear deformation plate theory. Applied Mathematical Modelling 2011;35:708-727.

[42] Liew KM, Hung KC, Lim MK. A continuum three-dimensional vibration analysis of thick rectangular plates. International Journal of Solids and Structures 1993;30:3357-3379.

[43] Malik M, Bert CW. Three-dimensional elasticity solutions for free vibrations of rectangular plates by the differential quadrature method. International Journal of Solids and Structures 1998;35:299-318.

Table Captions

Table 1. Deflections and stresses of SS plates under uniformly distributed loads

Table 2. Deflections $\hat{w}$ of rectangular plates with various boundary conditions under uniformly distributed loads ($b = 2a$)

Table 3. The first eight frequencies $\bar{\omega}$ of square SS plates

Table 4. Fundamental frequencies $\bar{\omega}$ of square and rectangular Levy-type plates

Table 1. Deflections and stresses of SS plates under uniformly distributed loads

b/*a*	*a*/*h*	Methods	$\bar{w}$	$\bar{\sigma}_x$	$\bar{\sigma}_y$	$\bar{\sigma}_{xy}$	$\bar{\sigma}_{yz}$	$\bar{\sigma}_{xz}$
1	5	ABAQUS	0.0536	0.2872	0.2872	0.1945		
		CPT [34]	0.0444	0.2873	0.2873	0.1946	0.4909	0.4909
		FSDT [34]	0.0536	0.2873	0.2873	0.1946	0.4909	0.4909
		TSDT [34]	0.0535	0.2944	0.2944	0.2112	0.3703	0.3703
		Present	0.0536	0.2942	0.2942	0.2125	0.4909	0.4909
	10	ABAQUS	0.0467	0.2872	0.2872	0.1945		
		CPT [34]	0.0444	0.2873	0.2873	0.1946	0.4909	0.4909
		FSDT [34]	0.0467	0.2873	0.2873	0.1946	0.4909	0.4909
		TSDT [34]	0.0467	0.2890	0.2890	0.1990	0.4543	0.4543
		Present	0.0467	0.2890	0.2890	0.1991	0.4909	0.4909
	100	ABAQUS	0.0444	0.2872	0.2872	0.1945		
		CPT [34]	0.0444	0.2873	0.2873	0.1946	0.4909	0.4909
		FSDT [34]	0.0444	0.2873	0.2873	0.1946	0.4909	0.4909
		TSDT [34]	0.0444	0.2873	0.2873	0.1947	0.4905	0.4905
		Present	0.0444	0.2873	0.2873	0.1947	0.4909	0.4909
2	5	ABAQUS	0.1248	0.6100	0.2794	0.2772		
		CPT [34]	0.1106	0.6100	0.2779	0.2769	0.5240	0.6813
		FSDT [34]	0.1248	0.6100	0.2779	0.2769	0.5240	0.6813
		TSDT [34]	0.1248	0.6202	0.2818	0.2927	0.4569	0.5615
		Present	0.1248	0.6201	0.2817	0.2934	0.5240	0.6813
	10	ABAQUS	0.1141	0.6100	0.2794	0.2772		
		CPT [34]	0.1106	0.6100	0.2779	0.2769	0.5240	0.6813
		FSDT [34]	0.1142	0.6100	0.2779	0.2769	0.5240	0.6813
		TSDT [34]	0.1142	0.6125	0.2789	0.2809	0.5051	0.6448
		Present	0.1142	0.6125	0.2789	0.2810	0.5240	0.6813
	100	ABAQUS	0.1106	0.6100	0.2794	0.2772		
		CPT [34]	0.1106	0.6100	0.2779	0.2769	0.5240	0.6813
		FSDT [34]	0.1106	0.6100	0.2779	0.2769	0.5240	0.6813
		TSDT [34]	0.1106	0.6100	0.2779	0.2769	0.5238	0.6809
		Present	0.1106	0.6100	0.2779	0.2769	0.5240	0.6813

Table 2. Deflections $\hat{w}$ of rectangular plates with various boundary conditions under uniformly distributed loads ($b = 2a$)

a/*h*	Methods	Boundary conditions					
		CC	SC	SS	FC	FS	FF
5	ABAQUS	1.0000	1.0703	1.1429	1.2089	1.2842	1.4280
	FSDT [37]	1.0000	1.0704	1.1430	1.2090	1.2844	1.4283
	Present	0.9357	1.0373	1.1430	1.1757	1.2849	1.4293
		(1.0186)*	(1.0799)		(1.2193)		
10	ABAQUS	0.8850	0.9637	1.0453	1.0980	1.1827	1.3225
	FSDT [37]	0.8850	0.9637	1.0454	1.0981	1.1829	1.3228
	Present	0.8673	0.9546	1.0454	1.0893	1.1834	1.3239
		(0.8902)	(0.9664)	1.0454	(1.1014)		
25	ABAQUS	0.8511	0.9329	1.0180	1.0663	1.1545	1.2935
	FSDT [37]	0.8511	0.9330	1.0181	1.0664	1.1547	1.2938
	Present	0.8481	0.9314	1.0181	1.0651	1.1550	1.2944
		(0.8519)	(0.9334)		(1.0671)		
1000	ABAQUS	0.8445	0.9270	1.0128	1.0604	1.1494	1.2884
	FSDT [37]	0.8445	0.9270	1.0129	1.0605	1.1496	1.2887
	Present	0.8445	0.9270	1.0129	1.0605	1.1496	1.2887
		(0.8445)	(0.9270)		(1.0605)		

* Deflection values obtained using Eq. (40) for the clamped boundary conditions.

Table 3. The first eight frequencies $\bar{\omega}$ of square SS plates

h/*a*	Methods	Modes							
		1	2	3	4	5	8	7	8
0.4	ABAQUS	13.7882	26.4265	26.4265	35.7317	40.9814	40.9814	47.9095	47.9095
	3D-Ritz [42]	13.9467	26.8986	26.8986	35.9915		-	-	- -
	TSDT [40]	13.8135	26.5907	26.5907	36.1316	41.5668	41.5668	48.8368	48.8368
	Present	13.7875	26.4215	26.4215	35.7266	40.9638	40.9638	47.8888	47.8888
0.3	ABAQUS	15.5628	31.5525	31.5525	43.7850	50.7798	50.7798	60.0619	60.0619
	3D-Ritz [42]	15.6877	31.9834	31.9834	44.5346	50.4850	50.4850		- -
	TSDT [40]	15.5742	31.6410	31.6410	44.0234	51.1315	51.1315	60.6546	60.6546
	Present	15.5619	31.5457	31.5457	43.7780	50.7550	50.7550	60.0430	60.0430
0.2	ABAQUS	17.4498	38.1621	38.1621	55.1615	65.1844	65.1844	78.7284	78.7284
	3D-Ritz [42]	17.5264	38.4826	38.4826	55.7870	65.9961	65.9961		- -
	3D-DQ [43]	17.5260	38.4827	38.4827	55.7871	65.9961	65.9961		- -
	FSDT [39]	17.5055	38.3847	38.3847	55.5860	65.7193	65.7193	79.4758	79.4758
	TSDT [40]	17.4524	38.1885	38.1885	55.2540	65.3131	65.3131	78.9864	78.9864
	Present	17.4486	38.1522	38.1522	55.1501	65.1453	65.1453	78.6970	78.6970
0.1	ABAQUS	19.0665	45.4972	45.4972	69.8139	85.1044	85.1044	106.7419	106.7419
	3D-Ritz [42]	19.0898	45.6193	45.6193	70.1038	85.4876	85.4876	107.3710	107.3710
	3D-DQ [43]	19.0901	45.6193	45.6193	70.1040	85.4878	85.4878	107.3695	107.3695
	FSDT [39]	19.0840	45.5845	45.5845	70.0219	85.3654	85.3654	107.1775	107.1775
	TSDT [40]	19.0651	45.4870	45.4870	69.8097	85.0641	85.0641	106.7350	106.7350
	Present	19.0650	45.4827	45.4827	69.7944	85.0380	85.0380	106.6836	106.6836
0.01	ABAQUS	19.7337	49.3208	49.3208	78.8686	98.6094	98.6094	128.0921	128.0921
	TSDT [41]	19.7320	49.3032	49.3032	78.8421	98.5169	98.5169	128.0024	128.0024
	Present	19.7320	49.3032	49.3032	78.8421	98.5169	98.5169	128.0024	128.0024
0.001	ABAQUS	19.7408	49.3651	49.3651	78.9823	98.7871	98.7871	128.3921	128.3921
	CPT [38]	19.7392	49.3480	49.3480	78.9568	98.6960	98.6960	128.3049	128.3049
	FSDT [39]	19.7391	49.3475	49.3475	78.9557	98.6943	98.6943	128.3019	128.3019
	TSDT [41]	19.7391	49.3475	49.3475	78.9556	98.6943	98.6943	128.3019	128.3019
	Present	19.7392	49.3476	49.3476	78.9557	98.6942	98.6942	128.3018	128.3018

Table 4. Fundamental frequencies $\bar{\omega}$ of square and rectangular Levy-type plates

b/*a*	*h*/*a*	Methods	Boundary conditions					
			CC	SC	SS	FC	FS	FF
1	0.4	ABAQUS	15.5633	14.6388	13.7882	9.3287	8.9910	7.7355
		TSDT [41]	15.9616	14.8301	13.8136	9.3654	8.9998	7.7394
		Present	14.7563	14.2636	13.7875	9.6589	9.4076	7.9366
	0.3	ABAQUS	18.5122	16.9610	15.5628	10.3291	9.8552	8.3807
		TSDT [41]	18.8246	17.0923	15.5745	10.3523	9.8591	8.3820
		Present	17.6212	16.5627	15.5619	10.6064	10.1868	8.5346
	0.2	ABAQUS	22.3632	19.7060	17.4498	11.3633	10.6996	8.9847
		3D-DQ [43]	22.6088	19.8505	17.5260	11.3982	10.7216	9.0011
		FSDT [39]	22.5099	19.7988	17.5055	11.3931	10.7218	8.9997
		TSDT [41]	22.5355	19.7695	17.4523	11.3736	10.7002	8.9840
		Present	21.5843	19.3878	17.4486	11.5726	10.9211	9.0817
	0.1	ABAQUS	26.6750	22.3924	19.0665	12.2509	11.3749	9.4424
		3D-DQ [43]	26.8089	22.4535	19.0901	12.2623	11.3953	9.4460
		FSDT [39]	26.7369	22.4260	19.0840	12.2606	11.3810	9.4458
		TSDT [41]	26.7084	22.4018	19.0651	12.2519	11.3737	9.4417
		Present	26.3327	22.2699	19.0650	12.3662	11.4742	9.4820
	0.01	ABAQUS	28.9324	23.6367	19.7337	12.6755	11.6771	9.6291
		FSDT [39]	28.9250	23.6327	19.7322	12.6728	11.6746	9.6270
		TSDT [41]	28.9241	23.6321	19.7320	12.6725	11.6740	9.6265
		Present	28.9202	23.6310	19.7320	12.6840	11.6824	9.6298
2	0.4	ABAQUS	9.9641	9.7377	9.5390	8.2246	8.1801	7.8188
		TSDT [41]	10.0164	9.7644	9.5472	8.2333	8.1855	7.8232
		Present	9.8068	9.6671	9.5380	8.3736	8.3349	7.9391
	0.3	ABAQUS	11.0996	10.7585	10.4705	8.9594	8.8964	8.4767
		TSDT [41]	11.1328	10.7736	10.4733	8.9634	8.8982	8.4779
		Present	10.9519	10.6952	10.4693	9.0791	9.0185	8.5698
	0.2	ABAQUS	12.2796	11.7774	11.3721	9.6601	9.5731	9.0909
		FSDT [39]	12.3152	11.8061	11.3961	9.6782	9.5902	9.1061
		TSDT [41]	12.2939	11.7827	11.3717	9.6606	9.5726	9.0899
		Present	12.1770	11.7357	11.3707	9.7407	9.6524	9.1499
	0.1	ABAQUS	13.2735	12.5941	12.0690	10.2010	10.0889	9.5527
		FSDT [39]	13.2843	12.6022	12.0752	10.2054	10.0929	9.5560
		TSDT [41]	13.2747	12.5937	12.0675	10.1997	10.0874	9.5554
		Present	13.2389	12.5802	12.0674	10.2371	10.1223	9.5765
	0.01	ABAQUS	13.6830	12.9168	12.3359	10.4227	10.2969	9.7349
		FSDT [39]	13.6815	12.9152	12.3343	10.4206	10.2948	9.7328
		TSDT [41]	13.6813	12.9151	12.3342	10.4206	10.2938	9.7322
		Present	13.6810	12.9150	12.3342	10.4235	10.2973	9.7346

Figure Captions

Fig. 1. Geometry and coordinates of a rectangular plate

Fig. 2. Comparison of fundamental frequencies $\bar{\omega}$ of SS square plates

Fig. 3. Comparison of deflections $\bar{w}$ of SS square plates

Fig. 4. Transverse shear stresses for SS plate strips under sinusoidal loads

Fig. 5. Deflections of Levy-type plates with $a/h = 0.1$ and $b = 2a$

Fig. 6. Mode shapes of SS square thick plates with $a/h = 0.4$

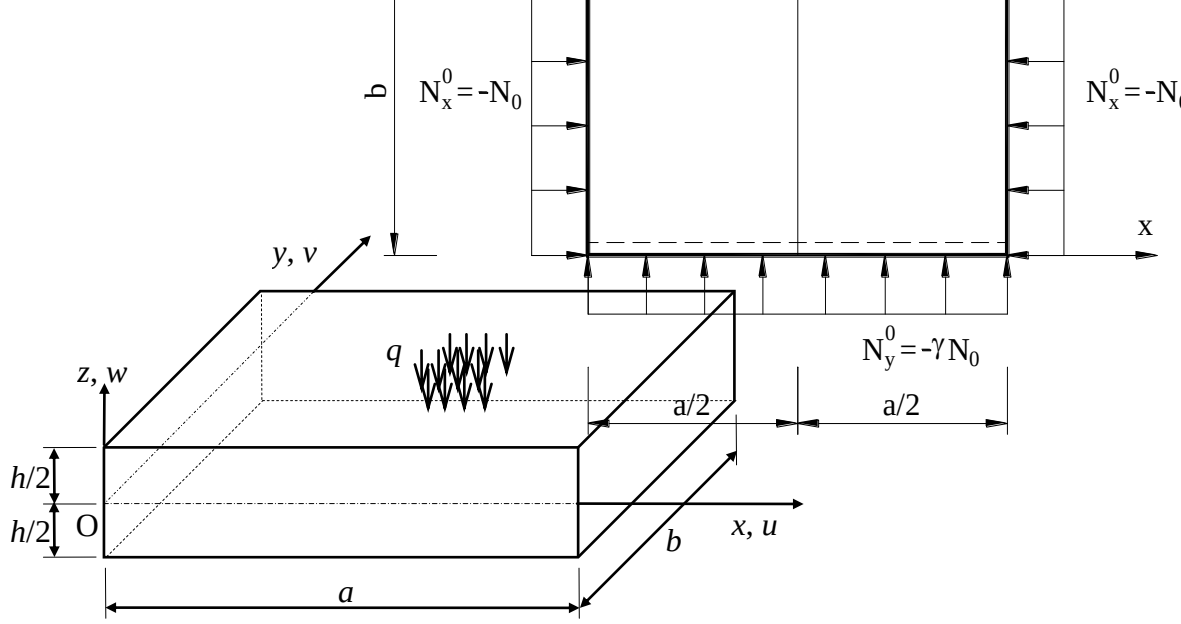

Fig. 1. Geometry and coordinates of a rectangular plate

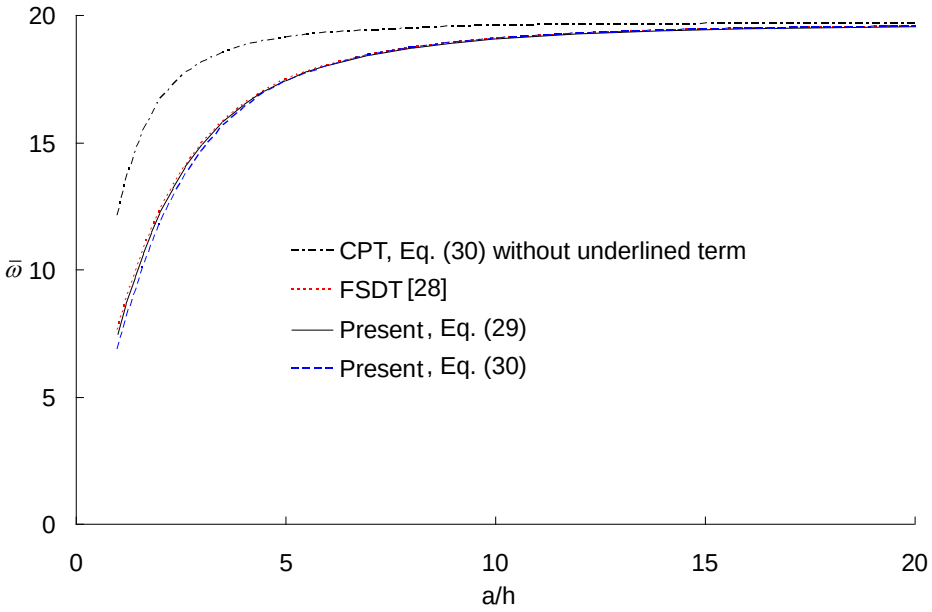

Fig. 2. Comparison of fundamental frequencies $\bar{\omega}$ of SS square plates

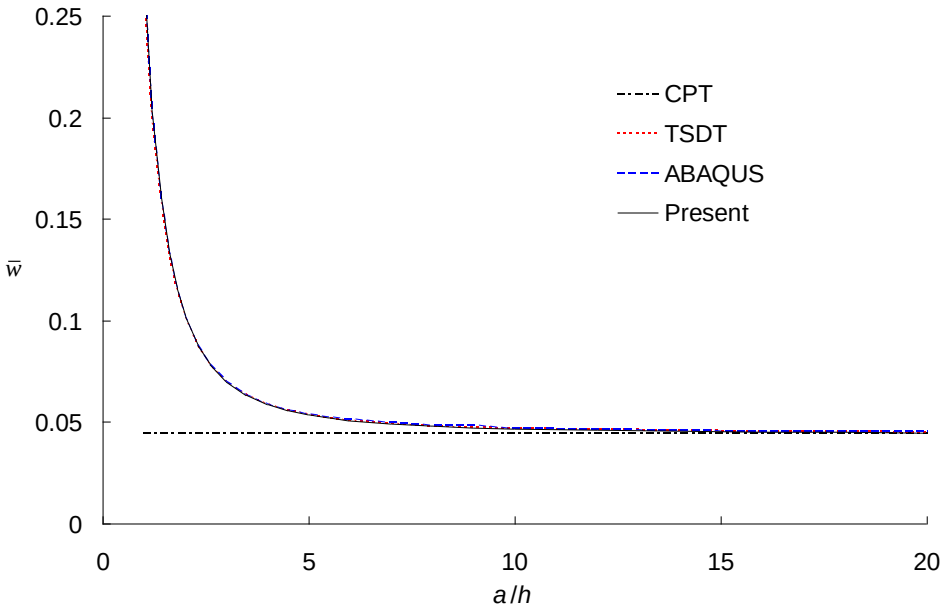

Fig. 3. Comparison of deflections $\bar{w}$ of SS square plates

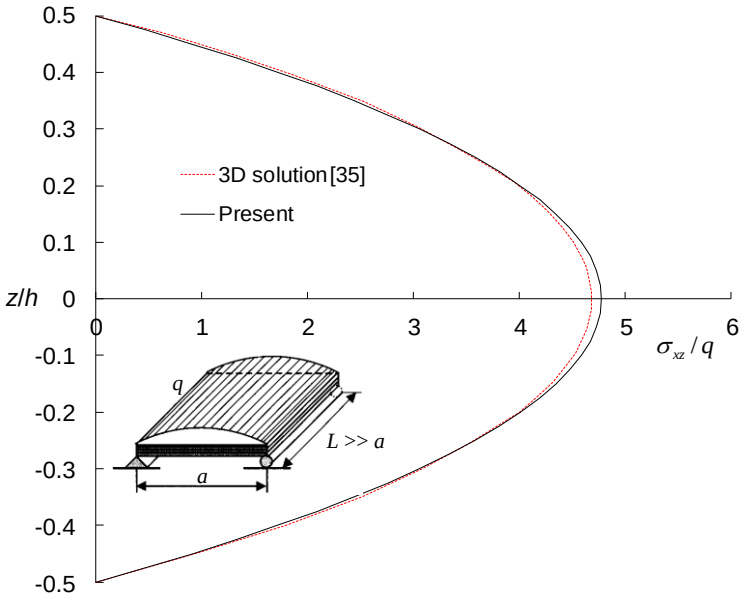

Fig. 4. Transverse shear stresses for SS plate strips under sinusoidal loads

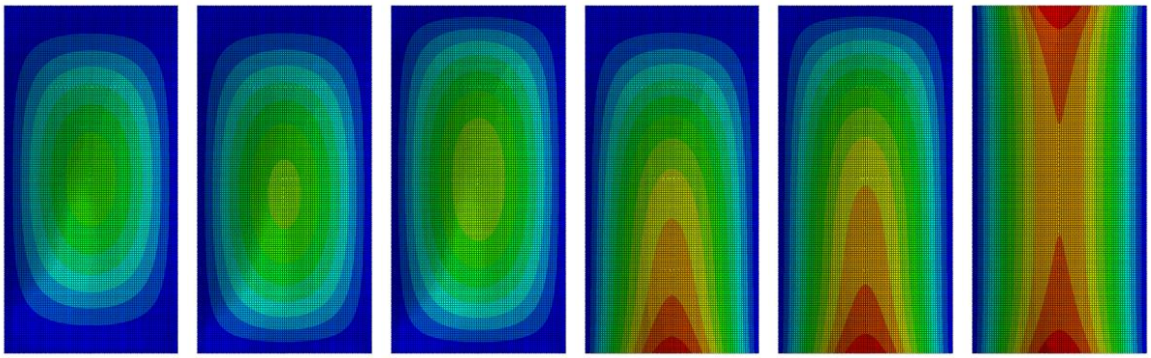

Fig. 5. Deflections of Levy-type plates with a/h = 0.1 and b = 2a

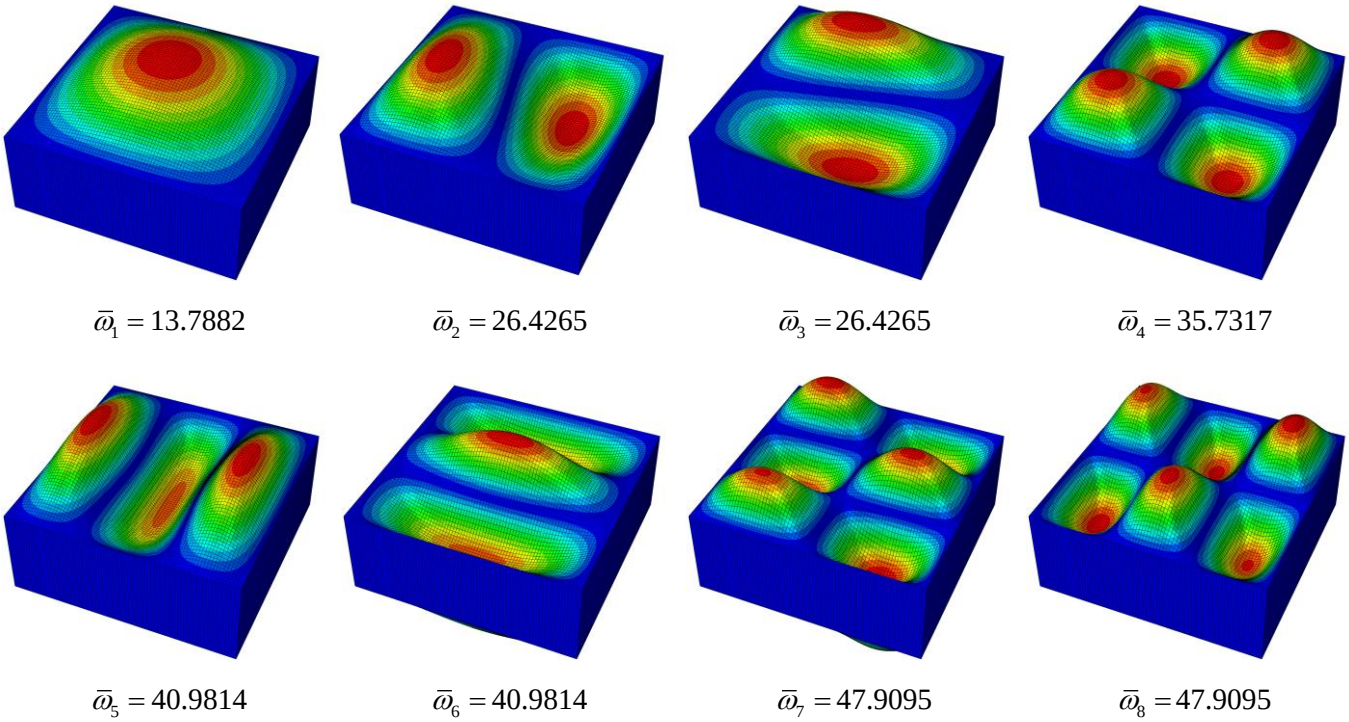

Fig. 6. Mode shapes of SS square thick plates with a/h = 0.4